Low Temperature Physics/Fizika Nizkikh Temperatur, 2020, v. 46, No. 3, pp. 328–335

# Graphenes and CNTs: adatoms, islands, nanocrystals, and intercalants as interacting multipoles

V.A. Lykah[1] and E.S. Syrkin[2]

[1]*National Technical University "Kharkiv Polytechnic Institute", 2 Kyrpychov Str., Kharkiv 61002, Ukraine*
E-mail: lykahva@yahoo.com

[2]*B. Verkin Institute for Low Temperature Physics and Engineering of the National Academy of Sciences of Ukraine*
*47 Nauky Ave., Kharkiv 61103, Ukraine*
E-mail: syrkin@ilt.kharkov.ua

Received October 28, 2019, published online January 27, 2020

The functionalization (adsorption) of graphene and carbon nanotubes (CNT) is investigated in the case of charge transfer between a functionalizing molecule (adatom) and a substrate (graphenes or CNT), and the first principles charge transfer calculations are briefly reviewed. It is shown that electrostatic dipoles caused by charge transfer describe the interaction between the adsorbed atoms or islands (clusters) at low concentration, that is, at the initial and intermediate stages of functionalization. It is shown that intercalated atoms in graphite, bi-, and tri-graphene can be described by the electrostatic quadrupoles, their magnitudes are found. The quadrupoles' axes are perpendicular to the layers. On the surface of the CNT, the adsorbed nanocrystals (clusters) are described as electrostatic quadrupoles, their magnitudes are found. The quadrupoles' axes are directed along the CNT. At long distances, the interaction energies and repulsion forces are calculated for the clusters. The results explain the experimentally found homogeneous distribution of the adsorbed particles and clusters.

Keywords: graphenes, graphite, carbon nanotubes, structure of adsorbates.

## 1. Introduction

Graphene is a single layer material consisting of carbon atoms. Since its discovery [1], graphene has attracted great interest due to its excellent electric field effect transport properties and massless Dirac fermions like charge carriers. The carbon nanotube (CNT) is graphene rolled into a cylinder and can be considered as quantum wire [2]. Functionalization is a powerful method for tuning Fermi level and quantum energy levels of 1D (CNT) and 2D (graphene, bigraphene) nanomaterials what modifies their physical properties. Review of organic and inorganic functionalization can be found in [3] for graphene and in [4] for CNT.

Homogeneouse, sometimes periodic, distribution of metallic, metal-organic [5] and conducting polymers [6] particles at CNT surface was found by TEM. The charge transfer [5] leads to electron and hole pairs appearing, which are spatially separated in neighboring substrate (CNT and a molecule or atom). Usually, the contributions from dispersion and valence forces [7] are the most important part of the interaction energy at short-range distances. The electrostatic components of the intermolecular interaction were considered in [7] for general case and in [8] for the adsorption case. In this treatment the classical multipole expansion [9,10] is used. In the work [11] and references therein, an electric dipole is considered as a generalization of the familiar phenomenon of the atomic collapse of single charged impurity to the case where electron-hole pairs are spontaneously created from vacuum in bound states with charge impurities thus partially screening them.

The first-principle calculations of the interaction between Li and graphene [12] considered the configurations and the concentration of Li adsorption. At low concentration, the 2s state of Li is *fully unoccupied due to the charge transfer*. With the increase of Li concentration, the 2*s* state is broadened and occupied partly by electrons.

The zero and finite temperature behavior of Li on graphene was studied by DFT and Monte Carlo techniques [13]. The calculations reveal two distinct types of orderings of Li on graphene, Li-gas (dispersed Li-ion) and Li-cluster, island, stripe phases. At the zero-temperature calculations show that the Li-graphene interaction is mainly electrostatic and phase separation to pristine graphene and bulk Li is energetically more favorable. However, at nonzero temperatures, the lesser-ordered Li-gas and Li-cluster states are more favorable at sufficiently low concentrations. In the

case of Li adatom, the electrons transferred to graphene are localized on the hexagon at the Li atom is adsorbed, *creating a net dipole*.

*Ab initio* study of potassium (K) adsorption on graphene and carbon nanotubes [14] reveals the large dipole moment normal to the surface and a significant charge transfer. It implies that the long-range K-graphene interaction appears to be predominantly ionic or electrostatic in nature. The estimations indicate that the effective amount of the *electronic charge transferred* from the K atom to the graphene surface increases with increasing the size of the supercell from 0.14 e to 0.70 e. A simple classical model allowed explaining the disagreement between the experimental and calculated interaction energies by long-range electrostatic interactions between potassium and graphene. In contrast, the energy of potassium adsorption on carbon nanotubes depends on the nanotube surface curvature and chirality [14].

The adsorption of 12 different metal adatoms from groups I–III of the Periodic Table on graphene was studied using first-principles density-functional theory [15]. From the density of states (DOS) and from charge-density integration, the charge transfer was found 0.14–0.9 e.

The ferric chloride $FeCl_3$ was used to intercalate graphite flakes consisting of 2–4 graphene layers and to dope graphene monolayers. The intercalant, staging, stability, and doping was characterized by Raman scattering [16]. They estimated a Fermi-level shift of $\simeq 0.9$ eV, corresponding to a charge transfer 0.152 holes per carbon atom.

It was reported [17], that the features of the Raman peak of few-layer graphene intercalation compounds (FLGIC) with $FeCl_3$ are in good agreement with the full intercalation structures. The first principle calculations further reveal that its band structure is similar to single-layer graphene but with a strong doping effect due to the charge transfer from graphene to $FeCl_3$. The successful fabrication of FLGIC opens a new way to modify properties of graphenes for fundamental studies and future applications. Chan *et al*. [18] reported the effect of (i) charge transfer, (ii) change of in-plane lattice constant and (iii) intercalate-coupling effect on the Raman-mode frequencies in graphite. In the charge transfer-induced doping effect [19] the graphene layer can be considered to be hole-doped since $FeCl_3$ is one of the acceptor-acceptor-type graphite bi-intercalation compounds [20].

In [19] Raman spectroscopy was used to investigate the interplay between surface adsorption and intercalation in few layer graphenes exposed to $Br_2$ and $I_2$ vapors at room temperature. Molecular intercalation into bulk graphite typically creates stable stoichiometric "stage" compounds (graphite intercalation compounds GICs). Bromine creates a stage bulk GIC in which graphene bilayers (2L) are separated by intercalated $Br_2$ layers. Such intercalated $Br_2$ layers are thought to be structurally commensurate with neighboring graphene. In contrast to $Br_2$, $I_2$ does not form a bulk GIC, possibly because the longer $I_2$ bond length does not allow an intercalation structure. $Br_2$ and $I_2$ are more electronegative than graphite and should dope graphene positively when adsorbed. $I_2$ adsorbs on and dopes carbon nanotubes and fullerenes. Charge transfer from the carbon substrate creates iodide anions that react with excess neutral $I_2$ to form adsorbed $I_3^-$, and $I_5^-$; these species are directly detected as resonantly enhanced Raman bands.

The model for the calculation of the *polarization properties* of $sp^2$ carbon materials and, in particular, fullerenes and carbon nanotubes was developed, see [21] and references within. This model describes the self-consistent interactions by both a net electric charge and a dipole originated from each carbon atom. The theory of the *polarons* in the functionalized semiconducting CNT was developed [22]. The theory is based on research of energy spectra tuning as result of functionalization of CNT and nanowires by layers of *polar molecules* with (i) radial degree of freedom [23], (ii) conformational transition in the molecules [24] and (iii) incommensurate periodic structures [25].

The aim of this work is theoretical consideration of initial stages of functionalization with the charge transfer between a molecule and substrate (graphenes or CNT). It is shown that the electron-hole pairs can be presented as the dipole and quadrupole moments with long-range interaction. We consider situation of enough small molecules (atoms) with relatively large distance between ones. This approach allows describing the long-range electrostatic interaction of the adsorbed or functionalizing molecules (atoms), their clusters [13,19] and nanobeads [5] at the graphene or CNT surface, and inside intercalated bigraphene and graphite. It is shown that the long-range electrostatic multipole potential leads to repulsion and homogeneous distribution of the functionalizing and intercalating molecules (atoms).

The considered multipoles' configurations and calculations are shown in the upper row and the left column of Table 1. The table has a structure of matrix where a cross-section of a column and a row represent number of the section that considers corresponding interaction or the multipole calculation in one of Appendixes A, B, C or D. Dash in matrix means absence of corresponding interaction or consideration.

At long-range distances, the proposed method describes the intermolecular interaction adequately. At short-range distances, compared with the molecules size, the proposed method would be applied with higher error because of the destroy of multipole approximation. Note that the dispersion

Table 1. The multipoles (upper row and left column) $d$, $Q_{\text{bead}}$, and $Q_{\text{intc}}$ (dipole, quadrupoles of nanobead and of intercalated atom) considered in the present paper (numbers mean section, "calc" means calculation of the multipole)

| Multipole | $d$ | $Q_{\text{bead}}$ | $Q_{\text{intc}}$ | calc |
|---|---|---|---|---|
| $d$ | 2 | 3.2 | 3.3 | A |
| $Q_{\text{bead}}$ | 3.2 | 3.1 | – | C |
| $Q_{\text{intc}}$ | 3.3 | – | 3.3 | D |
| calc | A | C | D | – |

and valence forces have higher powers $k$ in the dependence on distance ($\sim 1/R^k$), therefore, they begin to play the main role at short-range distances.

## 2. Dipoles at graphene and CNT

The charge transfer is an example of a general contact interaction of atoms or molecules with different electronegativity. Thus, in comparison with CNT and graphene as a molecule we have electronegative molecules $FeCl_3$ [17], $Br_2$, $I_2$ [19] and their complexes, adatoms F, Cl, O, N, P, S and electropositive metals or metal-organic complexes [5]. In further consideration we suppose the molecules (atoms) to be electropositive and the electronic clouds of the transferred charge to be negative. These situations are shown in Fig. 1. A dipole vector $\mathbf{d} = q\mathbf{r}$ is shown as arrow between centers of negative and positive charges in Fig. 1 (see Appendix A). Following to [7,9] we write dipole–dipole interaction as:

$$U_{dd} = \frac{d^2}{R^3}\left[(\boldsymbol{\omega}_1 \cdot \boldsymbol{\omega}_2) - 3(\boldsymbol{\omega}_1 \cdot \mathbf{n})(\boldsymbol{\omega}_2 \cdot \mathbf{n})\right], \qquad (1)$$

where $\mathbf{R} = \mathbf{R}_{12}$ is the radius-vector between centers of the dipoles 1 and 2, $R = |\mathbf{R}|$, the unit vectors $\boldsymbol{\omega}_1$, $\boldsymbol{\omega}_2$ and $\mathbf{n} = \mathbf{n}_{12}$ are directed along $\mathbf{d}_1$, $\mathbf{d}_2$ and $\mathbf{R}$. Relations like $(\boldsymbol{\omega}_1 \cdot \mathbf{n}) = \|\boldsymbol{\omega}_1\| \cdot \|\mathbf{n}\| \cos\theta$ mean the dot product between two vectors, where $\theta$ is the angle between them. Analogues relations describe interaction between dipoles $\mathbf{d}_1$, $\mathbf{d}_3$.

Force of interaction between two particles is

$$F_{ij} = -\frac{dU_{ij}(R)}{dR} = \frac{k}{R}U_{ij}(R). \qquad (2)$$

Here we use dependence of the potential of type $U_{ij}(R) \sim 1/R^k$. For example, in (1) the power $k = 3$ and $U_{ij} = U_{dd}$. Below in next formulae for $U_{ij} = U_{Qd}$ and $U_{QQ}$ the powers are $k = 4; 5$ correspondingly. The positive force $F$ means repulsion of the interacting particles.

Therefore in Fig. 1, the configuration of the dipoles gives $F_{12} > 0$ (repulsion) and $F_{13}, F_{23} < 0$ (attraction) according to (1), (2). The cause is the mutual orientation of the unit vectors in relation (1): perpendicular $(\omega_i \cdot \mathbf{n}) = 0$, parallel $\cos\theta_{12} = (\boldsymbol{\omega}_1 \cdot \boldsymbol{\omega}_2) > 0$, and antiparallel $\cos\theta_{13} = (\boldsymbol{\omega}_1 \cdot \boldsymbol{\omega}_3) < 0$, $\cos\theta_{23} = (\boldsymbol{\omega}_2 \cdot \boldsymbol{\omega}_3) < 0$. These orientations give the maximum value of the interaction. At CNT surface a turn of the dipole around the axis of the nanotube is possible. In the last case, the product of vectors can vary continuously between maximal and minimal values, and change its sign also.

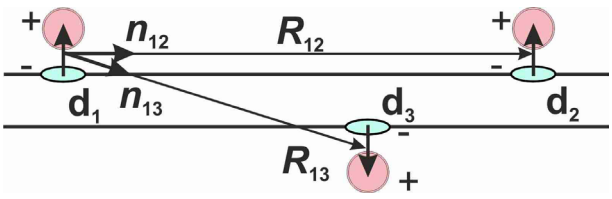


*Fig. 1.* (Color online) The functionalizing molecules or atoms (pink spheres, sign "+") at substrate (semiconducting CNT or bigraphene) with transferred electrons (blue ellipsoids, sign "–") create the dipoles $\mathbf{d}_1$, $\mathbf{d}_2$, $\mathbf{d}_3$. According to (1), (2), for long range dipole interaction, the parallel dipoles $\mathbf{d}_1 \| \mathbf{d}_2$ repel each other, and opposite ones $\mathbf{d}_1$, $\mathbf{d}_3$ attract.

For more general orientation of the dipole 2 between orientation 2 and 3 in Fig. 1 and in (1), (2), the boundary between attractive and repulsive orientation is defined by the equation

$$F_{dd} = 0. \qquad (3)$$

Increasing the functionalizing molecules concentration leads to the formation of different clusters or islands [5,6,13,19] which can't be described in the present model. Only the small clusters which contain $N$ of the molecules or adatoms can be described by Eq. (1) applying $d \to d_N = Nd$ transformation. A renormalization of the charge transfer can depend strongly on the cluster size. Thus, DFT and Monte Carlo techniques [13] give the dipole moment 0.802 eÅ for Li adatom and 0.247, 0.077, 0.125, 0.119, and 0.096 eÅ for 2, 3, 4, 5, and 6 Li clusters, respectively.

## 3. Electric quadrupoles in the functionalized and intercalated carbon systems

### *3.1. Nanobeads at CNT as the quadrupoles*

The nanobeads, nanospheres, and nanocrystals are formed at the CNT or nanowire surface [5,6] at higher concentration of the functionalizing molecules. These structures have almost periodic or periodic fragments with period ~ 10–50 nm, see straight line segments of CNT in [5, Figs. 15, 16, 18], [26, Figs.5 b, c], [27, Figs. 3 c, f, 4 c]. Sometimes the nanobeads are so narrow (see [5, Fig. 18] that rather can be named as a nanoring or a fasten nanobelt. The chemical treatment provides a stronger interaction CNT–$RuO_2$ and a more uniform dispersion along the side (see [5, Fig. 18]. The minimal size nanobeads (nanorings) are schematically depicted in Fig. 2.

We propose to describe the nanobeads with charge transfer between a molecule and substrate as electric quadrupole, see Appendix B. Following to [7], quadrupole-quadrupole interaction $U_{QQ}$ is:

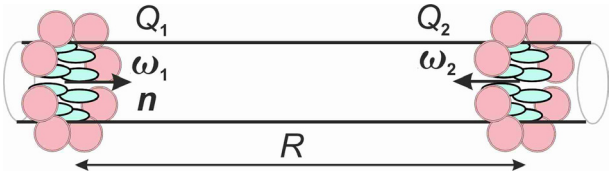


*Fig. 2.* The quadrupoles $Q_1$, $Q_2$ are formed by the nanobeads of the adsorbed metal atoms or metal-organic molecules at the CNT surface. The quadrupoles repel each other according to (4), (5).

$$U_{QQ} =$$

$$= \frac{3Q^2}{4R^5}\Big[1-5(\boldsymbol{\omega}_1\cdot\mathbf{n})^2-5(\boldsymbol{\omega}_2\cdot\mathbf{n})^2+2(\boldsymbol{\omega}_1\cdot\boldsymbol{\omega}_2)^2+$$

$$+35(\boldsymbol{\omega}_1\cdot\mathbf{n})^2(\boldsymbol{\omega}_2\cdot\mathbf{n})^2-20(\boldsymbol{\omega}_1\cdot\mathbf{n})(\boldsymbol{\omega}_2\cdot\mathbf{n})(\boldsymbol{\omega}_1\cdot\boldsymbol{\omega}_2)\Big]. \quad (4)$$

Here $Q$ is the nanobead's quadrupole moment (see Appendix C and Fig. 6), $R$ is the distance between centers of both quadrupoles in Fig. 2, $\mathbf{n}$, $\boldsymbol{\omega}_1$, $\boldsymbol{\omega}_2$ are unit vectors: $\mathbf{n} \parallel \mathbf{R}$ and directions of $\boldsymbol{\omega}_1$, $\boldsymbol{\omega}_2$ are along the corresponding quadrupole axes.

In Fig. 2 and relation (4), the unit vectors $\boldsymbol{\omega}_1$, $\boldsymbol{\omega}_2$ are directed along the quadrupoles' axes and are collinear to $\mathbf{n}$. Then in the case of two nanobeads, we have the interaction energy $U_{QQ} = 6Q^2 / R^5 > 0$ and force

$$F_{QQb} = \frac{30Q^2}{R^6} > 0, \quad (5)$$

according to relation (2). It means *two nanobeads repulsion* due to interaction between the created electrostatic quadrupoles. In combination with a boundary condition at the CNT ends, this quadrupole-quadrupole repulsion corresponds to the experimentally observed uniform (periodic or almost periodic) distribution of the nanobeads, nanospheres, and nanocrystals [5].

### *3.2. Nanobeads and adsorbed atoms (quadrupoles and dipoles) at CNT*

Dipole-quadrupole interaction energy is [7]:

$$U_{Qd} = -\frac{3Qd}{2R^4}[(\boldsymbol{\omega}_1\cdot\mathbf{n})+$$

$$+2(\boldsymbol{\omega}_1\cdot\boldsymbol{\omega}_2)(\boldsymbol{\omega}_2\cdot\mathbf{n})-5(\boldsymbol{\omega}_1\cdot\mathbf{n})(\boldsymbol{\omega}_2\cdot\mathbf{n})^2]. \quad (6)$$

Here $R$ is distance between centers of the dipole $d$ $(\boldsymbol{\omega}_1 \parallel \mathbf{d})$ and the quadrupole $Q(\boldsymbol{\omega}_1 \perp \boldsymbol{\omega}_2)$ in Fig. 3, $\mathbf{n}$, $\boldsymbol{\omega}_1$, $\boldsymbol{\omega}_2$ are unit vectors. At large distances, the mutual orientations are following: $\boldsymbol{\omega}_2 \parallel \mathbf{n} \parallel \mathbf{R}$.

For the dipole and quadrupole in Fig. 3, the unit vectors are perpendicular $\boldsymbol{\omega}_1 \perp \boldsymbol{\omega}_2$. Then the dipole–quadrupole force is:

$$F_{Qd} = -\frac{6Qd}{R^5}(\boldsymbol{\omega}_1\cdot\mathbf{n})[1-5(\boldsymbol{\omega}_2\cdot\mathbf{n})^2] \simeq +\frac{24Qd}{R^5}(\boldsymbol{\omega}_1\cdot\mathbf{n}),$$

$$|(\boldsymbol{\omega}_1\cdot\mathbf{n})|_{R\gg R_{NW}} \to 0, \quad (7)$$

$$|(\boldsymbol{\omega}_2\cdot\mathbf{n})|_{R\gg R_{NW}} \to 1,$$

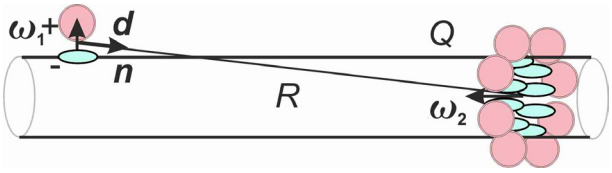


*Fig. 3.* Interacting of the dipole $\mathbf{d}$ of a metal adatom and the quadrupole $Q$ formed by a metallic nanobead are shown at the CNT surface according to (6).

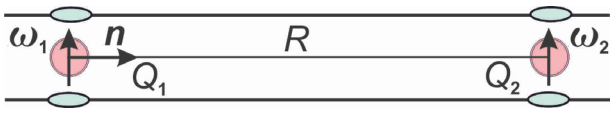


*Fig. 4.* The quadrupoles formed by the intercalating molecules (atoms) repel each other inside bigraphene. The unit vectors $\boldsymbol{\omega}_1$, $\boldsymbol{\omega}_2$ show the quadrupoles' axes.

where $R_{NW}$ is the nanowire (CNT) radius, see Fig. 6. According to (2), (6), and (7) at large distances, an *indifferent equilibrium* of the dipole between two nanobeads $F_{Qd} \to 0$ exists, see Eqs. (6), (7). If orientations of the unit vectors, see Fig. 3 and Eq. (7), give $(\boldsymbol{\omega}_1\cdot\mathbf{n}) < 0$ and $|(\boldsymbol{\omega}_1\cdot\mathbf{n})| \ll 1$ then very weak dipole–nanobead attraction (unstable equilibrium) is possible. At the middle-range distances $R \sim R_{NW}$, the quadrupole approximation for the nanobeads is not valid. It seems that we must consider an interaction between an individual dipole of an adatom and individual dipoles of the nanobead. We have the dipole–dipole repulsion. At the short distances $R \sim R_{\text{at}}$ we have the main interatomic attraction by short-range forces: valence, dispersive, etc. The periodic arrangement of the nanobeads [5] is experimentally observed. It indicates that the thermal motion of the adatoms easily overcomes the potential barriers near the nanobeads.

### *3.3. Quadrupoles for intercalated bigraphene and graphite*

Another case of quadrupoles formation is intercalation into bigraphene or graphite, see Fig. 4, Appendix D, and Fig. 6. It seems, to provide the charge transfer into two planes it would be better to have higher valence of intercalating atoms (molecules). The axes of symmetry of these quadrupoles are perpendicular to the graphitic layers and are mutually parallel. Therefore, the following relations are satisfied $(\boldsymbol{\omega}_1\cdot\boldsymbol{\omega}_2)^2 = 1$ and $(\boldsymbol{\omega}_1\cdot\mathbf{n}) = (\boldsymbol{\omega}_2\cdot\mathbf{n}) = 0$ where a unit vector $\mathbf{n}$ is shown in Fig. 4. Therefore, from relations (2), (4) we obtain

$$F_{QQ_{\text{intc}}} = \frac{45Q^2}{4R^6} > 0. \quad (8)$$

It means repulsion of two intercalated particles.

In the case of the semiconducting bigraphene, an adsorbed atom (molecule) is possible at external surface, see Fig. 1, and an intercalated atom between the layers, see Fig. 4. Then the *dipole and quadrupole* can interact, see Fig. 5. In the case of metallic bigraphene or graphite such electrostatic

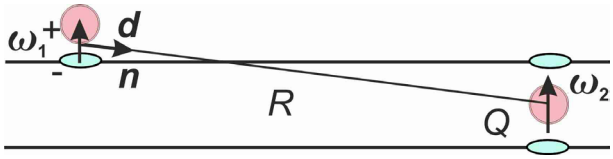


*Fig. 5.* Interaction of the adatom's dipole and quadrupole formed by the intercalating atom in semiconducting bigraphene according to (9).

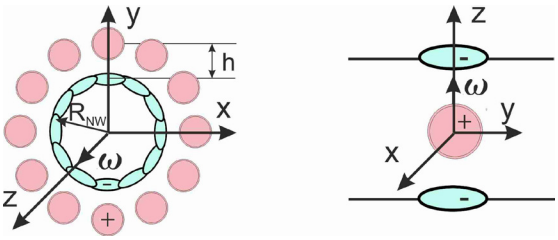


*Fig. 6.* To an explanation of the quadrupole moments calculation: the functionalizing atoms in the nanobead (left) and the intercalated atom in bigraphene (right) are shown. The unit vector **ω** shows direction of the quadrupole moment axis.

interaction is screened by the conducting graphitic layer. For the comparison in Fig. 2, the carbon nanotube has known type of conductivity which depends on the chirality.

In Figs. 2–4, orientations of the quadrupoles are different. We try to keep the notation in formulas and Fig. 5. The unit vectors are collinear $\boldsymbol{\omega}_1 \| \boldsymbol{\omega}_2$ Then the dipole–quadrupole force is:

$$F_{Qd_{\text{intc}}} = -\frac{6Qd}{R^5}(\boldsymbol{\omega}_1 \cdot \mathbf{n})[3-5(\boldsymbol{\omega}_2 \cdot \mathbf{n})^2] \simeq$$

$$\simeq -\frac{18Qd}{R^5}(\boldsymbol{\omega}_1 \cdot \mathbf{n}); \quad |(\boldsymbol{\omega}_1 \cdot \mathbf{n})|_{R\to\infty} \to 0. \qquad (9)$$

Therefore, at large distances, the interaction disappears. At very small distances, the multipole approximation is not valid. At intermediate distances, the dispersion and valence forces [7] are compared with electrostatic ones (9). An additional analysis is necessary.

### 4. Discussion and conclusion

In this article we have used the model proposed in the experimental works [5]: the charge transfer between the substrate and the adsorbed (functionalizing) atoms exists. The model of the charge transfer is based on spectroscopy (see [5] and references therein), Raman spectroscopy [16,17,19], and the first principle calculations [12–17]. It is naturally, that formation, growth, and rearrangement of the arising charged clusters in an adatoms gas require some exposition time. We considered the middle and low-temperature limit when the electron is localized near an adsorbed particle that is a source of the transferred charge. The space distribution of the charges, transferred to the substrate and rested near the adsorbed ion, is described in approximation of the electrostatic multipoles. In this case, the geometry and local concentration of the adsorbed particles play an important role.

It seems, that the dipole description of the adsorbed atoms is applied too widely [8,11]. The dipole moment is the first term in the multipole expansion [9,10]. Here we have shown that at one plane (metallic or semiconductor) the adsorbed particles are repulsed. Meanwhile, at different sides of thing semiconductor plane (bigraphene) the adsorbed particles are attracted.

At the semiconductor nanowire surface, in the case of the charge transfer, the interaction between the adsorbed particles depends on the mutual dipoles orientation: attraction (antiparallel) and repulsion (parallel) in the far distance. The intermediate orientations and distances need more detail analysis, general description is written in relation (1). For the limit cases of small and large distances, the results are given by relations (3). The metal nanowire surface screens electric field and needs more complicated analysis at general dipole orientations.

For the CNT or nanowire with adsorbed atoms and the charge transfer, it is shown that the nanobeads formation leads to the electrostatic quadrupole formation, see Fig. 2. It is shown that the axial symmetry of the nanobead's quadrupoles allows to describe their interaction in the terms of the unit vectors, see Fig. 2 and Eq. (4). In the terms of the long-range interaction (4) of the electrostatic quadrupoles, the coaxial nanobeads repel each other always what correlates with the experimentally observed almost periodic arrangement of the nanobeads [5]. In the real systems the nanobead are too massive objects which are product of the aggregation of the adsorbed atom (molecules). In our model we consider the minimal nanobeads with one atomic (molecular) row. These model nanobeads are unstable but, they correctly describe the interaction between the nanobeads. Transition to description of the real massive nanobeads can be reduced to the renormalization of $Q$ and $R_0$ values in the Ex. (4).

At the CNT surface, another interesting result is obtained for the interaction nanobead–adsorbed atom, i.e., quadrupole–dipole (6). At large distances this interaction comes to zero (7) due to the mutual orientation and arrangement of the quadrupole (nanobead) and dipole (atom) axes; the unit vectors are perpendicular. At the middle distances the perpendicularity is slightly broken and shallow barrier or attraction can arise. At atomic distances, attraction and atomic condensation at the nanobead surface becomes. It seems that even the potential barrier can be overcome easily by atomic thermal motion or the dipoles' repulsion. The experimental photos (see [5] and references therein) show the massive nanobeads and free nanowire surface between them.

Another type of quadrupole moments arises at intercalation of atoms (molecules) into bigraphene, threegraphene, and graphite. A metallic atom is electropositive in the pair metal–carbon, so the intercalating atom easy transfer it's electron or electrons to a graphitic layers, see Fig. 4. At intercalation, these quadrupole moments have different geometry and sign in comparison with the nanobeads at CNT. Repulsion between the quadrupoles exists in both cases (the nanobeads and the intercalated atoms). These quadrupole interactions are described by the same formula (4), but geometry is essential. Under intercalation, experimental observation of atomic periodic or almost periodic structures in a layer [5,28] is easily explained by repulsion.

**Acknowledgements**

This research was supported by the National Academy of Sciences of Ukraine (grant 4/18-H) and the Ministry of Education and Science of Ukraine (project M05486).

## Appendix A. The electric dipole

According to definition [9], the electrostatic dipole is vector:

$$\mathbf{d} = q\mathbf{r}. \tag{A1}$$

Here $q$ is a point charge of positive and negative parts. In the considered system, $q$ is the charge transferred from the metallic atom (metalorganic molecule) to the substrate (nanowire or plane). Vector $\mathbf{r}$ is directed from the negative to positive charge, i.e., goes from the surface to the metallic atom, see geometry in Fig. 1. If the metallic atom is at distance $h$ from the surface, then Eq. (A1) takes the following scalar view $d = qh$. Estimates can be made for the following parameter values: $q \simeq e, 2e$; $h \sim a \sim 0.3$ nm. Then for the adsorbed atom, the dipole value can reach $d \simeq qh \simeq ea \simeq$ $\simeq (4.8-9.6)\cdot 10^{-29}$ C·m which corresponds to experimental evaluation [13].

## Appendix B. The electric quadrupole

Following [7,9,10], an interaction with a complicated charge distribution in space is described by a multipoles. A multipole expansion is a mathematical series representing a function that depends on angles on a sphere combined with an expansion in radius. The first (the zeroth-order) term in the multipole expansion is called the monopole moment or charge $q$, the second (the first-order) term is called the dipole moment $\mathbf{d}$, the third (the second-order) is called the quadrupole moment (tensor $Q_{ij}$), the fourth (third-order) term is called the octupole moment [9,10], and the fifth (fourth-order) term is called the hexadecapole moment. Given the limitation of Greek numeral prefixes, terms of higher-order are conventionally named by adding "-pole" to the number of poles — e.g., 32-pole (rarely dotriacontapole or triacontadipole) and 64-pole (rarely tetrahexacontapole or hexacontatetrapole).

So, definition of tensor of the electric quadrupole moment is [7,9,10]:

$$Q_{ab} = \sum q\left(x_a x_b - \frac{1}{3}r^2\delta_{ab}\right), \tag{B1}$$

where $q$ is electric charge in point with coordinates $x_a, x_b$. In the main axes and after normalization $\mathrm{Tr}Q_{aa} = 0$ in the axially symmetric case, the quadrupole moment tensor is described by only one parameter $Q$ called the quadrupole moment [7,9]. Namely, the axially symmetric direction shows the vector of the quadrupole moment in the interactions formulae and figures [7]. The quadrupole moment vector is included in even powers into the interactions; therefore, the vector direction is indifferent along the axially symmetric direction. In Fig. 2 and left Fig. 6 external arrangement of the positive ions gives $Q > 0$, i.e., *the positive quadrupole moment*. According to definition (B1), the more is distance of the charge from the axes the more is contribution into the quadrupole moment $Q$. The positive metal ions are at larger radii than the negative transferred charges inside or at the CNT surface. In the case of the electronegative molecules adsorption, the nanobeads are negative and give the *negative quadrupole moment*.

## Appendix C. The quadrupole moment of the nanobead

Let us find the quadrupole moment of the nanobead which is formed by positive metal ions adsorbed at a nanowire surface, see Figs. 2 and 6. In the main axes, the axially symmetric contribution consists of two terms:

$$Q_{zz+} = qN(R_{NW}+h)^2; \quad Q_{zz-} = -qNR_{NW}^2. \tag{C1}$$

according to definition (B1), namely, the first term. Here $q$ is positive charge of the adsorbed atom, $R_{NW}$ is the nanowire radius, and $h$ is the distance between the adsorbed atom and the nanowire surface. Here we suppose set of the $N$ adsorbed atoms as point charges at the nanobead–nanowire surface.

For another main axes, components of the quadrupole moment tensor are

$$\begin{aligned} Q_{xx+} = Q_{yy+} &= \frac{1}{12}qN\left[6\left(R_{NW}+h\right)^2 + H^2\right], \\ Q_{xx-} = Q_{yy-} &= -\frac{1}{12}qN\left[6R_{NW}^2 + H^2\right]. \end{aligned} \tag{C2}$$

Here we have used results for moment of inertia of the thing hollow cylinder with height $H$ [29]. In our case, $H$ is the nanobead length along the nanowire. It is possible because of general construction of the quadrupole moment $Q_{ab}$ in (B1) without normalization is similar to the moment of inertia formula $J_{ab} = mx_a x_b$.

Let us write the second term in (B1) for the negative components:

$$(1/3)\mathrm{Tr}Q_{ii-} = -(2/3)qNR_{NW}^2 - H^2/18.$$

For the positive terms, the contribution has to be written in the same way with replacement $R_{NW} \to R_{NW} + h$. Finally, for the nanobead, the quadrupole moment tensor components are

$$\begin{aligned} Q_{xx} = Q_{yy} = \\ = \frac{1}{6}qN\left[-\left(R_{NW}+h\right)^2 + R_{NW}^2\right] = \\ = -\frac{1}{6}qN\left(2R_{NW}h + h^2\right), \\ Q_{zz} = \\ = \frac{1}{3}qN\left[\left(R_{NW}+h\right)^2 - R_{NW}^2\right] = \frac{1}{3}qN\left(2R_{NW}h + h^2\right). \end{aligned} \tag{C3}$$

Contribution of $H$, the nanobead length along the nanowire, does not manifest because the same size for positive

and negative charges. In the case of some charge delocalization in the nanowire, dependence on $H$ will appear.

Finally, for the nanobead the quadrupole moment equals

$$Q_{\text{bead}} = Q_{zz} = \frac{1}{3} qNh\left(2R_{NW} + h\right) > 0. \qquad \text{(C4)}$$

## Appendix D. The quadrupole moment of the intercalated atom

Let us find the quadrupole moment of the intercalated positive metal ions in bigraphene or graphite, see Figs. 4 and 6. In the main axes, the axially symmetric contribution consists of two terms:

$$\begin{aligned} Q_{zz+} &= q < R >^2 \to 0, \\ Q_{zz-} &= -q < R >^2 \to 0. \end{aligned} \qquad \text{(D1)}$$

according to definition (B1), namely, the first term. Here $q$ is positive charge of the adsorbed atom, $< R >$ is the average charge distribution radius. Here we suppose the atoms to be close to point charges that is $< R > \ll h$.

For another main axes, components of the quadrupole moment tensor are

$$\begin{aligned} Q_{xx+} = Q_{yy+} &= q < R >^2 \to 0, \\ Q_{xx-} = Q_{yy-} &= -qh^2, \end{aligned} \qquad \text{(D2)}$$

where $h$ is the distance between the intercalated atom and the graphene layer.

Let us write the second term in (B1) for the limit case of small charge sizes: $\text{Tr}Q_{ii-} = -qh^2$. Finally, for the intercalated atom, the components of the quadrupole moment tensor are

$$\begin{aligned} Q_{xx} = Q_{yy} &= \frac{1}{3} qh^2, \\ Q_{\text{intc}} = Q_{zz} &= -\frac{2}{3} qh^2 < 0. \end{aligned} \qquad \text{(D3)}$$

And in all previous formulae, the quadrupole moment for the intercalated atom equals $Q_{\text{intc}}$.


1. K.S. Novoselov, A.K. Geim, S.V. Morozov, D. Jiang, Y. Zhang, S.V. Dubonos, I.V. Grigorieva, and A.A. Firsov, *Science* **306**, 666 (2004).
2. C. Dekker, *Phys. Today* **52**, 22 (1999).
3. V. Georgakilas, M. Otyepka, A.B. Bourlinos, V. Chandra, N. Kim, K.C. Kemp, P. Hobza, R. Zboril, and K.S. Kim, *Chem. Rev.* **112**, 6156 (2012).
4. A. Hirsch and O. Vostrowsky, *Functionalization of Carbon Nanotubes,* in: *Functional Molecular Nanostructures*, A.D. Schlüter and K.N. Houk (eds.), Springer, Berlin, Heidelberg (2005).
5. D. Eder, *Chem. Rev.* **110**, 1348 (2010).
6. S.J. Park, O.S. Kwon, J.E. Lee, J. Jang, and H. Yoon, *Sensors* **14**, 3604 (2014).
7. *Physics of Cryocrystals*, Yu.A. Freiman and V.G. Manzhelii (eds.), AIP-Press, New York (1997).
8. D. Nicholson and N.G. Parsonage, *Computer Simulation and the Statistical Mechanics of Adsorption*, Academic Press., London, New York, Paris (1982).
9. L.D. Landau and E.M. Lifshits, *The Classical Theory of Fields*, Pergamon, Oxford, New York, Toronto (1975).
10. J.D. Jackson, *Classical Electrodynamics*, John Wiley & Sons, New York (1999).
11. E.V. Gorbar, V.P. Gusynin, and O.O. Sobol, *EPL* **111**, 37003 (2015).
12. G. Yang, X. Fan, Z. Liang, Q. Xu, and W. Zheng, *RSC Adv.* **6**, 26540 (2016).
13. Yu. Shaidu, E. Kucukbenli, and S. De Gironcoli, *J. Phys. Chem. C* **122**, 20800 (2018).
14. A. Lugo-Solis and I. Vasiliev, *Phys. Rev. B* **76**, 235431 (2007).
15. K.T. Chan, J.B. Neaton, and M.L. Cohen, *Phys. Rev. B* **77**, 235430 (2008).
16. Weijie Zhao, Ping Heng Tan, Jian Liu, and Andrea C. Ferrari, *J. Am. Chem. Soc.* **133**, 5941 (2011).
17. D. Zhan, L. Sun, Z.H. Ni, L. Liu, X.F. Fan, Yu.T. Wang, Y.M. Lam, W. Huang, and Z.X. Shen, *Adv. Funct. Mater.* **20**, 3504 (2010).
18. C.T. Chan, K.M. Ho, and W.A. Kamitakahara, *Phys. Rev. B* **36**, 3499 (1987).
19. N. Jung, N. Kim, S. Jockusch, N.J. Turro, P. Kim, and L. Brus, *Nano Lett.* **9**, 4133 (2009).
20. T. Abe, M. Inaba, Z. Ogumi, Y. Yokota, and Y. Mizutani, *Phys. Rev. B* **61**, 11344. (2000).
21. A. Mayer, *Phys. Rev. B* **75**, 045407 (2007).
22. V.A. Lykah and E.S. Syrkin, *Polarons in the Functionalized Nanowires*, in: *Polarons: Recent Progress and Perspectives*, A. Laref (ed.), Nova Science Publishers, New York (2018).
23. V.A. Lykakh and E.S. Syrkin, *Cond. Matter Phys.* **7**, 805 (2004).
24. V.A. Lykakh and E.S. Syrkin, *Ukr. J. Phys.* **57**, 710 (2012).
25. V.A. Lykah and E.S. Syrkin, *Adv. Optoelectronic Matter.* **1**, 25 (2013).
26. B. Jia, L. Gao, and J. Sun, *Carbon* **45**, 1476 (2007).
27. Y. Zhang, N.W. Franklin, R.J. Chen, and H. Dai, *Chem. Phys. Lett.* **331**, 35 (2000).
28. M.S. Dresselhaus and G. Dresselhaus, *Adv. Phys.* **51**, 1 (2002).
29. R.A. Serway and J.W. Jewett, Jr., *Physics for Scientists and Engineers with Modern Physics*, 7th Ed., Thomson and Brooks/Cole, Australia, Brazil, Canada, Mexico, Singapore, Spain, United Kingdom, United States (2008).

## Графени та ВНТ: адатоми, острівці, нанокристали та інтеркалянти як мультиполі, що взаємодіють

В.О. Ликах, Є.С. Сиркін

Функціоналізацію (адсорбцію) графену та вуглецевих нанотрубок (ВНТ) досліджено у випадку перенесення заряду між молекулою (адатомом), яка функціоналізує, та субстратом (графенами або ВНТ). Розглянуто розрахунки переносу заряду з перших принципів. Показано, що електростатичні диполі, які обумовлені перенесенням заряду, описують взаємодію між адсорбованими атомами або острівцями (кластерами) при низькій концентрації, тобто на початковій та проміжній стадії функціоналізації. Показано, що у графіті, бі- та тригафенах інтеркальовані атоми можна описати електростатичними квадруполями. Обчислено величину цих квадруполів та показано, що їх осі спрямовані нормально до шарів. На поверхні ВНТ адсорбовані нанокристали (кластери) описуються як електростатичні квадруполі. Величину цих квадруполів обчислено та показано, що їх осі спрямовані уздовж ВНТ. На великих відстанях розраховано енергії взаємодії та сили відштовхування кластерів. Результати пояснюють однорідний розподіл адсорбованих частинок та кластерів, що виявлено експериментально.

Ключові слова: графени, графіт, вуглецеві нанотрубки, структура адсорбатів.

## Графены и УНТ: адатомы, островки, нанокристаллы и интеркалянты как взаимодействующие мультиполи

В.А. Лыках, Е.С. Сыркин

Функционализация (адсорбция) графена и углеродных нанотрубок (УНТ) исследуется в случае переноса заряда между функциолизирующей молекулой (адатомом) и субстратом (графенами или УНТ). Рассмотрены расчеты переноса заряда из первых принципов. Показано, что электростатические диполи, обусловленные переносом заряда, описывают взаимодействие между адсорбированными атомами или островками (кластерами) при низкой концентрации, т.е. на начальной и промежуточной стадиях функционализации. Показано, что в графите, би- и тригафенах интеркалированные атомы можно описать электростатическими квадруполями. Вычислена величина этих квадруполей и показано, что их оси направлены нормально к слоям. На поверхности УНТ адсорбированные нанокристаллы (кластеры) описываются как электростатические квадруполи. Вычислена величина этих квадруполей и показано, что их оси направлены вдоль УНТ. На больших расстояниях рассчитаны энергии взаимодействия и силы отталкивания кластеров. Результаты объясняют обнаруженное экспериментально однородное распределение адсорбированных частиц и кластеров.

Ключевые слова: графены, графит, углеродные нанотрубки, структура адсорбатов.